Land Subsidence:
The Forgotten Enigma of Groundwater (Over)Extraction

Ariel Dinar[1], Encarna Esteban[2], Elena Calvo[2], Gerardo Herrera[3],
Pietro Teatini[4], Roberto Tomás[5], Yang Li[1], and Jose Albiac[6]

[1]University of California, Riverside, USA, Corresponding Author adinar@ucr.edu; [2]University of Zaragoza, Spain; [3]Geological Survey of Spain, Madrid (IGME); [4]University of Padova, Italy; [5]University of Alicante, Spain; [6]Agrifood Research and Technology Centre of Aragón (CITA), Zaragoza, Spain.

Abstract: Depletion of groundwater resources is currently one of the main environmental problems worldwide. The major groundwater systems on earth face large overexploitations with serious associated quality and quantity problems. Impacts of groundwater depletion involve serious economic damages from declining water tables, damages to linked groundwater-ecosystems, and consequences of water quality deterioration. However, during recent years another problem related with groundwater depletion has been gaining importance and attention—land subsidence that occurs in areas with specific geological characteristics in association with groundwater exploitation. Despite the large socio-economic impacts of land subsidence most of its effects are still not well analyzed and not properly recognized and quantified. We collected information on land subsidence from 119 sites around the world and, in the absence of quantified estimates, developed a land subsidence extent index. Then, we demonstrated qualitatively, using three case studies, the interaction between water extraction, land subsidence and their damages, and policy interventions to address it and their relative success. The overall results from the three case studies suggest that the effectiveness of policy intervention is determined by local conditions, including governance and regional economic development. Finally, we develop an optimization model of water extraction under conditions of land subsidence. The model is characterized by two sub problems corresponding to the phase before and after the occurrence of land subsides. The theoretical results suggest that the level of land subsidence impacts on both infrastructure and economic activities, and its impact on loss of storage capacity affect the behavior of the optimal path of the model, which tries to minimize such negative impacts. The extreme cases of very high values of these two impacts, trigger the model to prevent any irreversible damage (either in land subsidence impacts or in loss of storage capacity) by downscales extractions to the level that they will not affect land subsidence and remain within sub-problem 1.

Keywords: land subsidence; groundwater; water overdraft; two-stage optimization; Pontryagin backward-solving problem.
JEL Classification: Q25, Q56.
Acknowledgements: The authors were inspired by a session on Land Subsidence at the Rosenberg International Forum, San Jose, California, USA, October 7-10, 2018, dedicated to Sustainable Groundwater Management. Funding for part of the analysis in this paper was provided by the Giannini Foundation of Agricultural Economics. Ariel Dinar would like to acknowledge support from the W4190 Multistate NIFA-USDA-funded Project, "Management and Policy Challenges in a Water-Scarce World". Roberto Tomás would like to acknowledge support from the Spanish Ministry of Economy and Competitiveness, the State Agency of Research and the European Funds for Regional Development under project TEC2017-85244-C2-1-P. Roberto Tomás, Gerardo Herrera and Pietro Teatini acknowledge the EU support from the RESERVOIR project developed in the framework of the PRIMA programme.

Introduction

Land subsidence (LS) is the settlement of the land surface triggered by human-induced and natural-driven processes, such as natural compaction of unconsolidated deposits, or human activities such as sub-surface water mining, or fluids extraction (oil, gas and groundwater). Land subsidence is a global problem, mostly studied and recognized, to different extents, in association with aquifer over-exploitation. LS occurrence around the world is most prominent in those aquifers composed of loose unconsolidated materials (e.g. sands, clays, silts, etc.) that are over pumped (Gambolati and Teatini, 2015). For example, forty-five out of fifty states in the US have experienced varying degrees of land subsidence and 80% of the documented cases are due to groundwater extraction (CBWM Program Overview, 2019).

It is assessed that LS causes significant damages on local communities and on the environment (Yoo and Perrings, 2017). As such, identifying the types of damages and quantifying them both in terms of the various physical impacts and their economic values, short- and long-term, would be an essential first step for preparing policies to address the problem.

Most studies on LS are indicative in the sense that they identify the driving processes and measures the land subsidence amount and extent them in a specific locality. Few are the works that assess the impacts of LS in terms of social, environmental and economic consequences. A review of existing literature suggests that impacts of LS include (e.g. Holtzer & Galloway, 2005; Lixin et al, 2010; Erkens et al., 2016): (a) geological-related damage that affect subsurface lateral/horizontal water flows; (b) hydrogeological damage resulting from ground failure and loss of groundwater storage; (c) groundwater contamination in relation to ground fissures caused by LS; (d) environmental damage such as reduced performance of hydrological systems, malfunctioning of natural drainage systems, or wider expansion of flooded areas; (e) socio-economic impacts such as structural damage to buildings and infrastructures; (f) saltwater contamination of soils resulting in decrease of farmland productivity and sea water intrusion in coastal aquifers (decrease of fresh-water availability); (g) increase of drainage costs in coastal low-lying zones; (h) impact on adaptation ability to climate change, such as the loss of the buffer value of groundwater in years of scarcity; and (i) loss of high-value transitional areas (e.g., saltmarshes); and (j) shift of land use to poorer activities (e.g., from urbanized zones to rice fields, from rice fields to fish and shellfish farms, from fish farms to waste-water ponds) (Heri et al., 2018).

Increasing water demands across the globe, led by climate change impacts and population growth, are expected to increase groundwater withdrawals, especially in arid and semi-arid regions and in developing countries. The expected overexploitation of aquifers will spread and exacerbate current and future damage from various LS impacts. In this context, a better knowledge of the impacts of LS and their economic consequences is urgently needed.

This paper consists of three parts. It starts with a meta-analysis/review of relevant literature on LS occurrence and quantification of its impacts in various locations around the world. In the absence of economic value of the LS-inflicted damage, we develop an index to assess the extent of LS impacts. This assessment allows the identification of different types of impacts in different locations and explain how physical conditions, institutions, social systems, and existing policies could mitigate the LS extent. The paper includes also more focused descriptions of the social and environmental consequences of LS in a set of three case studies in various countries. Finally, the paper develops a dynamic optimization model of water extraction under conditions of LS. The findings of this paper will be used as input for developing an economic framework that allows the evaluation of tradeoff between short-term benefits from groundwater use vs. longer-term social costs from LS damage, and prioritize policy interventions aimed at dealing with maximizing social net benefits from use of groundwater.

The LS Extent index (LSE)

Due to the nature of the information we extracted from all reviewed LS studies, and following the earlier discussion on the difficulties to compare extent of impacts within a LS site and across LS sites, we adopted and adapted the Qualitative Structural Approach for Ranking (QUASAR) method as explained in Galassi and Levarlet (2017), who applied an assessment scale ranging between -6 and +6. In social life cycle assessment (LCA), which is very similar to the assessment of the 10 attributes of LS, the use of ordinal scoring scales has become the common practice. As summarized by Arvidsson (2019:604) the common ordinal scales include, but are not limited to: (a) (0, 1, 3, 5, 7, 9) (Hosseinijou et al. 2014), (b) (low, medium, high, very high) (Martínez-Blanco et al. 2014), (c) (1, 2, 3, 4) (Ramirez et al. 2014) and (1, 2, 3, 4, 5, 6) (Ciroth and Franze 2011). Ordinal scale values are also transformed into integers at some point in the assessment (e.g. very high → 6). One more example, similar to our methodological ranking, was used in Fontes (2016), where the ordinal scale (+ 2, + 1, 0, − 1, − 2) is used for scoring. The individual impact scores can

then be aggregated by social groups of activities and then can be further weighted (to reflect social preferences) into aggregated scores by social, geographical, or size of the group overall score (Arvidsson 2019).

Our assessment model was developed as follows: Our literature review consisted of published titles that include "Land Subsidence impacts." During the review of the literature we identified impacts that were discussed by the authors of the reviewed LS papers. Each LS reviewed was associated with up to *N* impacts (in our case we identified *N*=8 in the papers reviewed). We found several analyses of the same LS site. Some of the analyses included subsets of the *N* impacts. Therefore, in these cases we combined the impacts from the various reports. Because no quantitative measurement was provided, we just marked whether or not an impact is mentioned and thus it can have either a 0 value of a value of 1 (No/Yes).

Let A_i be the impact *i*, $i = 1, \dots, N$ in a given site.

$$A_i = \begin{cases} 0 & if \text{ the LS impact } i \text{ has no effect} \\ 1 & if \text{ the LS impact } i \text{ has an effect} \end{cases} \quad \text{for } i = 1, \dots, N.$$

Then the total net effect (*NE*) of LS (or the composite impact) is

$NE = \sum_{i=1}^{N} A_i,$

with *NE* being an integer. Given the nature of the A_is we can expect that $0 \leq NE \leq N$. Then the LS extent index (LSE) is defined as LSE=*NE/N*. Note that $0 \leq LSE \leq 1$.

We assume that the more LS impacts are identified in a site, the larger is the overall impact of LS.[1] A map of all 119 sites that were identified in our literature review with LS impacts is presented in Figure 1.

[1] The lack of detailed information of the impact of LS of different study cases can lead to a bias in the evaluation of the index. That is, for some sites recorded in the database, the available information about land subsidence and its effects is very limited and this fact can introduce deviations in our calculations of the index.

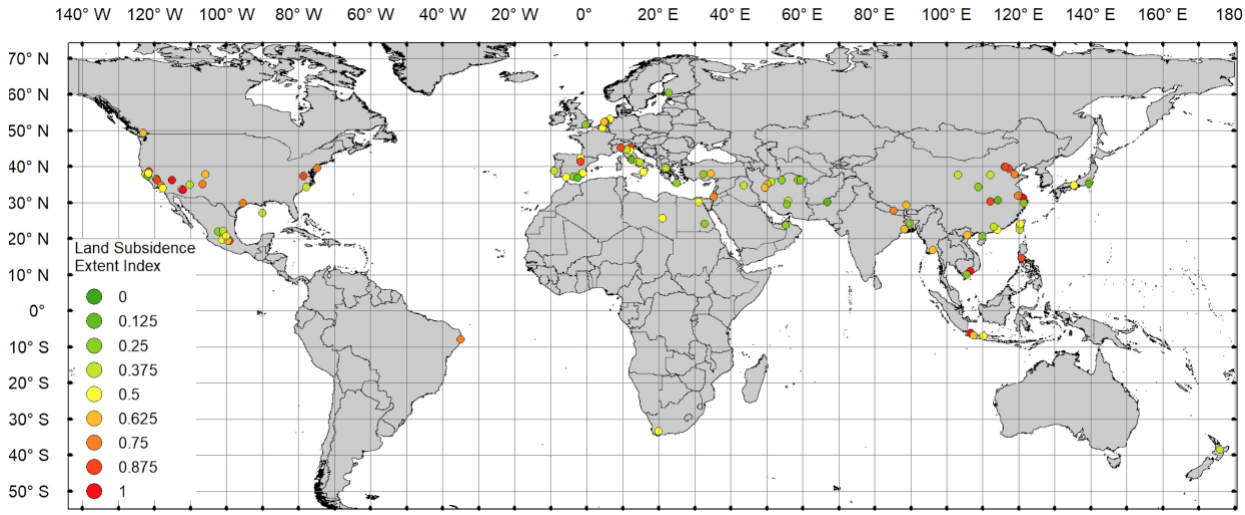

Figure 1: Global extent of land subsidence in a random literature review.

Source: Authors' elaboration.

Case Studies of LS-water extraction interaction and policy interventions

So far, we have been able to qualitatively assess the impacts of land subsidence, or at the most, count them. The second part of the paper provides three case study examples from three parts of the world on land subsidence occurrence, extent, effects, and policy interventions.

The Po River delta, Italy

Description of the region

The Po River in northern Italy, developed over the last few thousand years a delta stretching for 25 km, over a meridian arc of 90 km, spreading over 400 km2 (Figure 2(a)). The moderate rain precipitations (averaging 600 mm/year) and occasional snowfalls, the mild temperature, and abundant water availability have supported a flourishing agricultural sector that, in turn, has largely affected the conservation level of the region. The delta is characterized by the presence of a large system of shallow water bodies amounting to about 20,000 ha, half of which are natural lagoons (51%) and the remaining 49% are divided between regulated lagoons for aquaculture (43%) and wetlands (6%). Most of the delta lagoons are separated from the sea by barrier islands.

The sedimentary infill mainly consists of a succession of Messinian-to-Pleistocene deposits, generally characterized by a basin-scale tabular geometry and thicknesses of several hundred meters (Ghielmi et al., 2010). Active thrusts are buried beneath about 2000m thick Quaternary

sediments of Alpine and Apennine origin. The entire Quaternary sequence is composed of alternating continuous layers of sand and clay, almost normally consolidated and normally pressurized (Mattavelli et al., 1983), and a well-developed fresh-water multiaquifer system is located in the upper 400-500 m of the sedimentary sequence (Figure 2(c)) From 500yr B.P. to the second half of the 20th century, a sharp increase in the human intervention (i.e., river diversions, construction of artificial channels and dams, land reclamation) significantly affected the area. The delta prograde very rapidly, up to 200 m/yr, with a strong reduction in the coastal sand abundance and a thick mud deposition. More than a 25 m thickness of low consolidated sediments accumulated in the newer portions of the deltaic progradation, whereas in the ancient delta plain the thickness of the recent deposits amounted to a few meters only (Figure 2(c)).

Activities leading to LS

Land subsidence over the past century was monitored by levelling surveys using the benchmark network established by the Italian Military Geographic Institute at the end of the 1800s and then refined locally. More recently, the radar acquisitions by various satellites (ERS-1/2, ENVISAT-ASAR, COSMO-SkyMed, and ALOS-PALSAR) were processed through Synthetic Aperture Radar (SAR) interferometry. The loss of elevation between 1900 and 2015 is significant, with an average value of more than 1.5m and more than 3m in the inner part of the delta (Figure 2(b)) (Corbau et al., 2019).

The Po Delta experienced this dramatic subsidence due mainly to the large withdrawals of methane-rich groundwater, following World War II. Between the 1950s and the early 1970s, the extraction of natural resources led to a subsidence rates up to 300mm/yr over the period 1950–1957 in the more interior delta region where the main pumping centers were located.

LS effects

High rates of sea level rise between 1950s to 1970s led to geomorphological changes of the coastal systems and saltwater intrusion. These effects were enhanced by the reduction of sediment fluvial discharges, causing an intense erosion of the delta system (Correggiari et al., 2005). Land subsidence and the decrease of sediment availability made this territory particularly fragile (Simeoni and Corbau, 2009; Syvitski et al., 2009). Mostly after 1955, the shoreline significantly retreated and the nearshore slope increased. The subsidence was also responsible for the thinning and reorganization of the spits and the deepening of the lagoons.

At the same time, the high subsidence caused poor conditions for agriculture, with a great modification of the land use and cover in the Po Delta territory, specifically a drastic decrease of fruit trees, vineyards, and rice cultivations that were converted into less profitable crops such as corn, maize, and sugar beet.

The continuous loss of land elevation relative to the mean sea level (msl) dramatically increased the cost of keeping delta drained for agriculture practices. For example, only in the Veneto part of the studied area the energy consumption for pumping drainage water reached 4,335,297 kWh and 7,370,448 kWh in 1980 and 2017, respectively. The costs for maintaining the drainage systems also increased significantly.

Policies attempted to address the problems

The closure of the production wells by law in 1960 effectively decreased the subsidence rate. If the subsidence between 1957 and 1967 was still likely affected by the production peak occurred in 1959, a significant reduction of the subsidence rate since the late 1960s was observed.

Some residual land subsidence of anthropogenic origin is likely related to the delayed propagation of the piezometric decline in the fine-grained layers and viscous deformations typical of fine-grained soils (Isotton et al., 2019);

Although reduced with respect to the past, subsidence is still widespread today. Land settlement ranges from 1 to more than 15mm/yr with a general seaward increase. Land subsidence is now caused mainly by natural processes, i.e. the consolidation of Holocene deposits and, secondarily, of Quaternary sequence and tectonics (Teatini et al., 2011). Recent remote-sensing measurements show that the coastal strip is subsiding at rates many times faster than the Adriatic Sea level rise, recently quantified at 1.2 ± 0.1mm/yr (Carbognin et al., 2011).

Relative success of policies

The stop of groundwater withdrawals surely impacted positively in term of a drastic reduction of land subsidence rates. The present subsidence rates are returned to the values before the World War II. However, the damages caused by the past lowering cannot be recovered. Land subsidence has leaded to a decrease of water quality and quantity, the thinning of the unsaturated soil zone, and the desertification of some areas. Because of its elevation, largely below the mean sea level and only locally near or above the sea level, the delta is particularly vulnerable to weather and marine events. Water management will become even more important to keep the territory safe against floods from the sea, rivers or reclamation channels (Antonioli et al., 2017). The economic

activities, which mainly consist of crop production, require a permanent management of water surplus.

The lost elevation of the delta relative to the surrounding sea will never be recovered and the processes threatening the area will even worsen. The damages caused about 70 to 50 years ago cannot be anymore reversed. The recovery of the river transport of sediments toward the delta appears as the sole solution to mitigate the continuous decline in land elevation and reverse the shoreline erosion (Syvitski et al., 2009). An adaptation strategy proposed by Corbau et al. (2019) consists on restoration of transitional environments such as the swamps and salt marshes that were converted to farmlands in the past. This will allow to increase the resilience of the territory and, contemporary, reduce the management costs as larger portion of the delta will not be artificially drained through ditches and pumping stations.

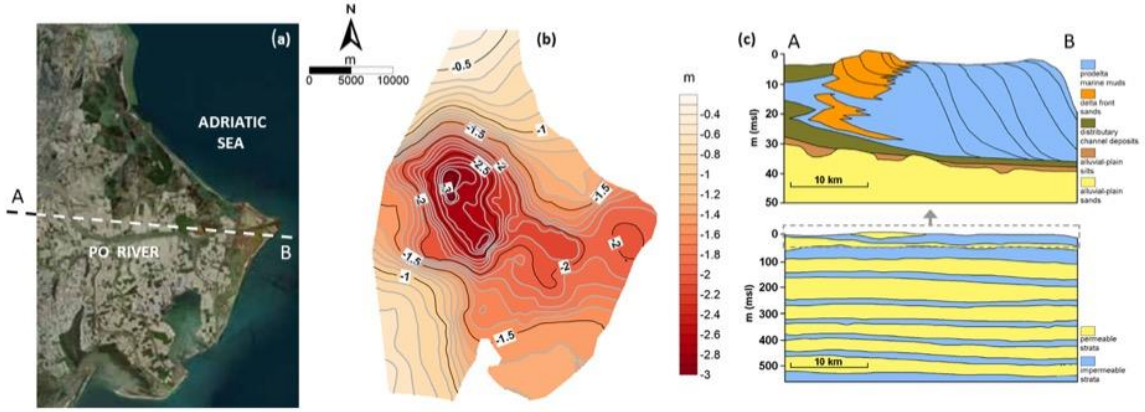

Figure 2: (a) Satellite view of present day Po Delta configuration; (b) cumulative land subsidence (m) over the period 1900 to 2015 (modified from Corbau et al., 2019); and (c) West-east cross section of the Po Delta subsurface along the AB alignment traced in (a) showing hydrogeological setting of the upper 500 m of the Quaternary deposit (bottom) and the lithostratigraphic section within the shallower 50m of the Late Pleistocene and Holocene sediments (top)

Source: Modified from Teatini et al., (2011).

The City of Murcia, Spain

Description of the region

Murcia is a city with over 400,000 inhabitants located in south-eastern Spain (Figure 3A). The city is placed within the Vega Media del Segura basin, confined within two mountain ranges to the north and south (Figure 3B). Segura river flows through the plain crossing the city to the east. Its

temperate climate with hot summers and very low precipitations, is responsible for drought periods triggering groundwater extraction from the aquifer system.

The city was developed over Plio-Quaternary alluvial loose deposits from the Segura river flood plain (Aragón et al. 2006; Mulas et al. 2003; Tomás et al. 2005)(Figure 3B). These deposits reach over 250m of thick and mainly fluvial and synsedimentary[2] alluvial fan deposits along the north and south borders of the basin (Figure 3C). From a hydrological point of view two aquifer units can be identified (Aragón et al. 2006): first a shallow semiconfined aquifer 3-30m thick of clay, silt and fine sand with a low conductivity, and second, a deep aquifer unit mainly characterized by the existence of alternations of fine (clay, silt and fine sand) and coarse (gravel) layers with a thickness of up to 200m and a conductivity three times greater than of the shallow aquifer unit.

Activities leading to LS and LS effect

During the 1990s, this area was affected by a drastic drought period that increased groundwater withdrawals from the aquifer system and led to a groundwater level drop of 15m. The intensive groundwater abstraction caused land subsidence resulting in 300 building complaints and damages of nearly 50 million euro (Mulas et al. 2003). Land sinking of nearly 10cm were measured between 1993 and 2004 using SAR Interferometry (Herrera et al. 2009b; Tomás et al. 2005). A second drought period was recorded between 2004 and 2008 with piezometric level drops of over 12m and land sinking of up to 8cm (Tessitore et al. 2016; Tomás et al. 2011). It is worth noting that during this second drought period, number of land subsidence events were lower and no specific building complaints or generalized damages were reported. This is probably due to soil pre-consolidation that occurred during groundwater level drop in the first drought period (Tomás et al. 2007).

Policies attempted to address the problems

Land subsidence triggered by groundwater pumping during drought periods in the 90s decade, raised the awareness of regional authorities, water management agencies and central government, leading to adoption of remedial policy measures and considering new tools for a sustainable exploitation of the aquifer system. In order to do so, a commission was promoted by the Regional Government to characterise and monitor subsidence in Murcia, and to evaluate subsidence impact. The Geological and Mining Survey of Spain was commissioned to monitor groundwater level by

[2]That forms or accumulate during sedimentation, i.e. fluvial and alluvial sediments accumulate at the same time.

a set of piezometers installed in the 1990s, monitoring land subsidence since 2001 through the combination of a network of more than 40 extensometer boreholes (Pardo et al. 2013) and satellite radar interferometry (Herrera et al. 2009a). This monitoring data have been used to implement hydrological and geotechnical models that simulate the behaviour of the aquifer system in the past drought periods (Herrera et al. 2009a; Tessitore et al. 2016; Tomás et al. 2010). Based on the available monitoring data and the developed numerical models, the Geological Survey of Spain and the University of Alicante have been providing advice to the groundwater management authorities of Segura Basin to achieve a sustainable exploitation of the aquifer system water.

Between 2005 and 2009 the water management authorities of the basin created clusters of deep pumping wells in order to increase the availability of groundwater resources to complement hydrological deficit and to coordinate the water extraction with the other hydrologic resources of the basin. The environmental declaration published in the State Official Newsletter (BOE 257, 25th October 2011, Sec III 16725) specified control actions and thresholds to ensure the sustainable exploitation of the aquifer system including: a maximum pumping volume of 48hm^3 per well (hm=hectometre=1000m^3), a maximum subsidence of 2 cm/year, ensuring that the floodable area in Norias Meander does not decrease more than 10%, and monitoring the piezometric levels every 15 days to ensure that they do not drop below historical minimum levels. Pumping of these wells is made by the Groundwater authority and a technical commission composed of experts from the local government, the Geological Survey of Spain and the River Basin Authority, ensures that the environmental impact declaration is fulfilled.

Relative success of policies

In Murcia city the combined action of the National, regional and groundwater authorities has permitted to firstly identify and understand subsidence hazard temporal and spatial distribution in the urban fabric, to understand the governing mechanisms and to implement advanced numerical models that simulate aquifer behavior in different pumping scenarios. These scientific and technical effort has permitted to propose a sustainable exploitation of the aquifer system that has been resumed in the Environmental declaration act, minimizing the impact in urban structures and infrastructures at present.

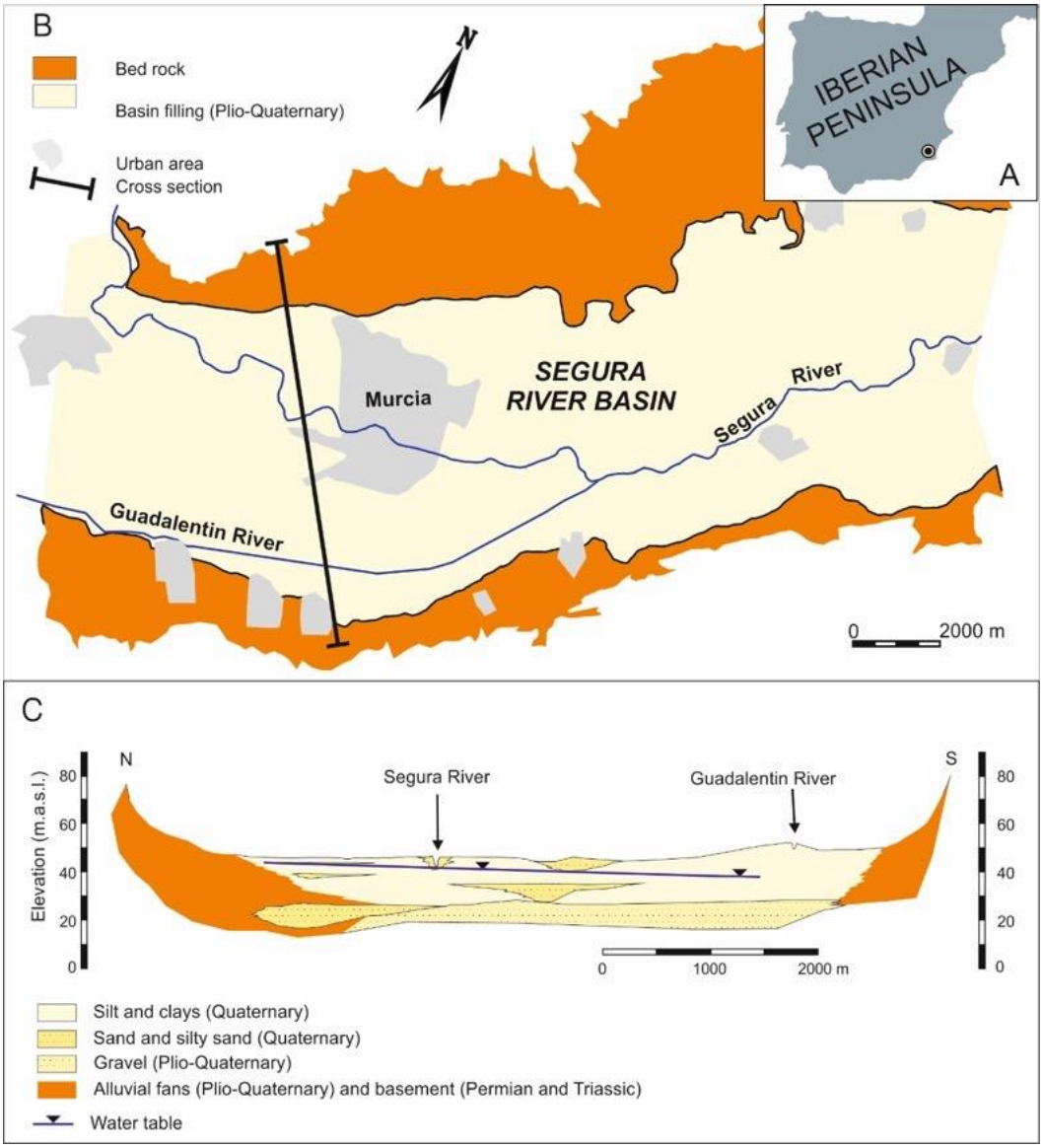

Figure 3: (A) Location of the study area. (B) Simplified Geological map of the Vega Media of the Segura; (C) Geological cross section across the basin (see location of the cross section in Figure 3B).

Source: Based on IGME (2000).

Chino Basin, California

Description of the Region

The Chino Basin, otherwise known as the Upper Santa Ana Valley, was formed from tectonic activities around major fault lines in Southern California. This basin is a part of a larger alluvial valley bordered by the San Bernardino Mountains to the north and the San Jacinto Mountains to the south. The Chino Basin hosts the Santa Ana River, which is not considered perennial. The Chino Basin is one of the largest groundwater basins in Southern California, containing approximately 5,000,000 acre-feet[3] of water and has an unused storage capacity of approximately 1,000,000 acre-feet. The basin consists of approximately 235 square miles of the upper Santa Ana River watershed and lies within portions of San Bernardino, Riverside, and Los Angeles counties (Wildermuth, 2005; CBWM, 2002).

The Chino Basin area includes a number of major faults. Namely, the Cucamonga Fault Zone, the Rialto-Colton Fault, the Red Hill Fault, the San Jose Fault and the Chino Fault. These faults were responsible for the formation of the depression of the Chino Basin area where the impermeable sedimentary and igneous bedrock formation formed the base of the freshwater aquifer. The sediments deposit which formed the reservoirs for groundwater in the area are greater than 1,000ft[1] thick at the deepest portion of this basin. Additionally, the major faults in the region serve as barriers of groundwater flow within the aquifer sediments and thus effectively serve as the boundaries and fulcrums of land subsidence events (CBWM, 2003). The groundwater in the Chino Basin came from three different sources. Some of the water enter the basin by infiltration of surface-water runoff from the highlands, by deep penetration of rain on the valley floor, and by artificial means such as irrigation return or induced recharge. The main directions of groundwater movement are southward from the mountains and westward from the adjacent basin (French, 1999).

Land Subsidence in the Chino Basin

The earliest evidence of land subsidence occurred in the form of ground fissures in the City of Chino in 1973 and have accelerated after 1991. The ground fissuring in the region have resulted in damage to the existing infrastructure. The Optimum Basin Management Program (OBMP) Phase 1 report of 1999 have identified the pumping-induced drawdown and subsequent aquifer-system compaction as the most probable cause of land subsidence and ground fissuring in

[3] 1 acre-foot=1235 m[3]; 1 foot=0.305 m.

Management Zone 1 (MZ-1). The 2005 investigation report states that groundwater production from deep and confined aquifer system in this area bore the greatest responsibility in stressing the aquifer system through inelastic (permanent) compaction of the aquifer-system sediments (Wildermuth, 2002; Wildermuth, 2005).

The effects of land subsidence in MZ-1 has been studied in great details via remote sensing. The inelastic compaction of the sediment during the 1987-1995 period is estimated at about 2.2 feet on average. The maximum level of land subsidence of 2.5 feet was observed at the City of Chino during this study (Figure 4 for the southwestern MZ-1). The surveys of the Chino Basin during the 1990s have also revealed the basin-wide oscillating (elastic) uplift and subsidence of the ground surface. This elastic ground movement is especially pronounced in the northern and eastern parts of the basin. Additionally, the City of Chino have experienced persistent and concentrated differential subsidence along the Central Avenue area. This area is coincident with a recurrently active ground surface fissure zone that has been discovered in 1973 with significant differential subsidence in this zone, especially in the periods before 1995. Additionally, InSAR (Interferometric Synthetic Aperture Radar) surveys of the area indicate that the faults are acting as barriers to groundwater flows in the area and will thus act as a fulcrum in the event of differential subsidence (CBWM MZ-1 Land Subsidence Management Plan, 2007).

Policy Interventions

With the rapid urbanization of the Inland Empire region, in which the Chino Basin resides, and the corresponding increase in water use, the Chino Basin Water Master (CBWM) was established per the 1978 Judgement by the Superior Court of the State of California for the County of San Bernardino. The CBWM was charged to develop the Optimum Basin Management Program (OBMP) on the use of the Basin. The OBMP Phase I (1999) report have identified that pumping-induced groundwater-level decline and the subsequent aquifer-system compaction as the most likely cause of the land subsidence and ground fissuring observed in MZ-1. The OBMP called for the development and management plans to minimize the subsidence and fissuring in MZ-1 in the short term, to collect and analyze the data on the mechanism and the rates of the subsidence, as well as to develop and implement a long-term management strategy for this issue. The initial phase of the MZ-1 was specific to the southwestern area of the zone (CBWM, 2002).

Data collection on the mechanism and the rate of land subsidence has been conducted through the use of extensometers in this area. The extensometer measures the rate of ground

material compaction and uplift at the different volumes of ground water pumping. This information would then be used to create a recommended level of pumping for all groundwater users in the basin. The CBWM will then report any instances of pumping above the recommended level by the users to the relevant authorities. The state of the MZ-1 along with recommendation for updates to the management plan will be published annually (CBWM, 2002; CBWM, 2007).

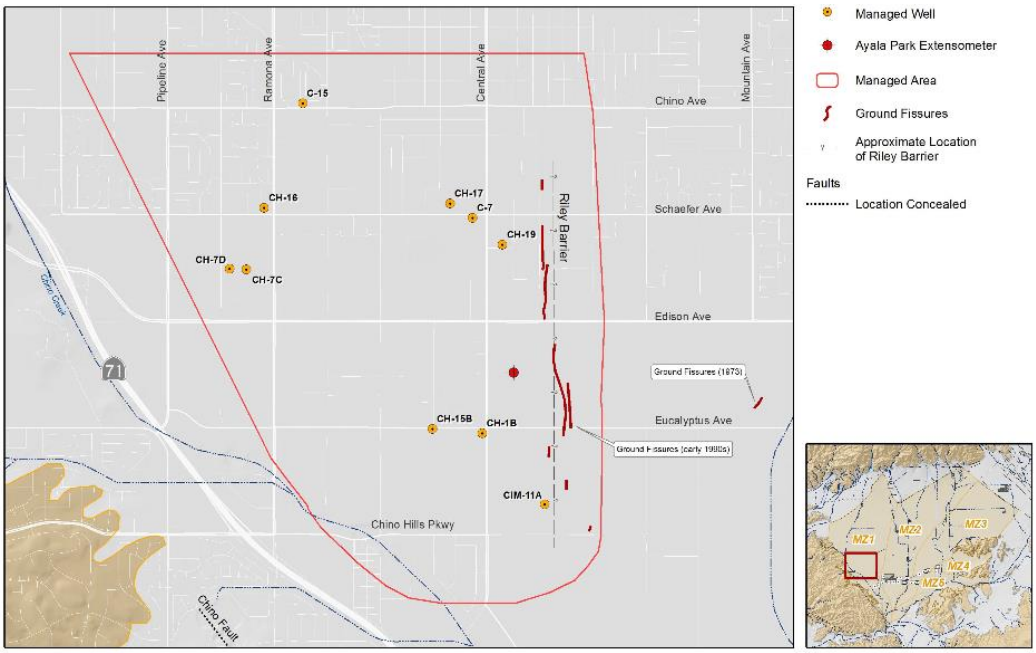

Figure 4: Southwestern MZ-1 in Chino Basin.

Source: Wildermuth Environmental Inc. (2018).

Relative success of policies

The controlled groundwater withdraws have been mostly successful. While the subsidence due to the permanent compaction of the sediment materials due to over pumping from the past decades cannot be reversed, the rate of change for land subsidence since the implementation of the management plan has been minimal (Figure 5, lower right panel). The controlled pumping according to the recommended levels (Figure 5, upper panel) and the recharging of aquifers have been effective in curtailing the draining of aquifers in MZ-1. No further instances of permanent compaction of the sediment layers were reported since 2012 and all vertical ground motions (Figure 5, Lower left panel) have been contained in the level that are considered to be elastic (Wildermuth, CBWM Land Subsidence Report, 2014-2017).

Additional recommendations have been included since 2013. While the control for permanent subsurface ground compaction has been mostly successful. The existence of ground faults at the edge of MZ-1 caused differential subsidence in areas immediately around the fault-lines. The differential subsidence is then manifested at the surface level in the form of ground fissuring. Due to the likelihood of infrastructure damage from ground fissuring, the MZ-1 management plan has called for the additional monitoring of ground fissuring near the in the form of elevation survey and electronic distance measurements (EDM) (WEI 2013, WEI 2015).

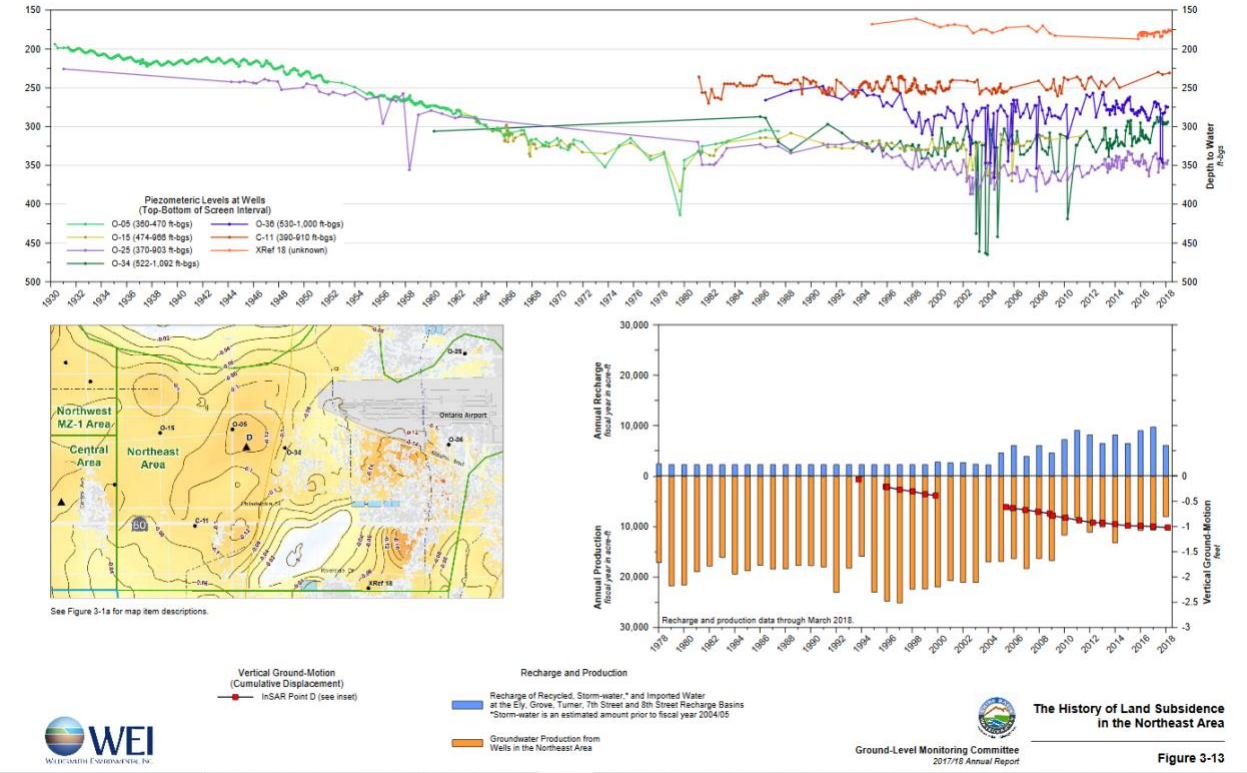

Figure 2: Recharge, extraction and vertical ground motion of Chino Basin, 2017.
Source: Wildermuth Environmental Inc. (2018).

The discussion so far suggests that there are major negative impacts of land subsidence on the affected regions (in the three case studies), depending on the geology of the aquifer. We are also aware that there are no economic estimates of land subsidence impacts, and how does land subsidence and ground water pumping interact and affect water use decisions. The next section is our contribution to the suggested dialogue on the forgotten effect of land subsidence on economic behavior of water users and other segments of society. The last part of the paper develops a dynamic economic model to optimize groundwater extraction in the presence of land subsidence.

Economics of groundwater management in presence of land subsidence

Land subsidence affects several economic activities and humans' quality of life. However, estimates of economic damages from land subsidence are not yet widely available and most of the published studies on land subsidence focus on a physical quantification of subsidence and on cataloguing the damages (Phantumvanit, 1989; Borchers and Carpenter, 2014). Some works have assessed local subsidence damages (Jones and Larson, 1975; Warren et al., 1975; Lixin et al., 2010; Yoo and Perrings, 2017; Wade et al., 2018). Selected damages cited in the literature range from $756 million in the Santa Clara Valley of California, in 2013 dollars (Borchers and Carpenter, 2014), to $1.3 billion in the San Joaquin Valley of California, between 1955-1972, in 2013 dollars, to $18.03 billion in the Tianjin metropolitan area in the period up to 2007 (Lixin et al., 2010).

The extent of social cost of land subsidence calls for society intervention in the form of regulation of groundwater pumping. In this context, groundwater optimal-control models should include land subsidence effects. So far, groundwater management models have not addressed land subsidence. Below, we propose a model where a social planner in charge of groundwater management accounts for the negative externalities of land subsidence due to aquifer depletion.

Traditional (social planner) representations of a groundwater model assume that a regulator pursues to maximize the net present value of a flow of future income from groundwater extractions:

$$(1) \quad SW = \int_{t=0}^{\infty} e^{-it}[B(W) - C(W,H)]dt$$

where the aggregated social welfare (*SW*) depends on private benefits from groundwater extractions *B*(*W*) minus the extraction cost *C(W, H)*, which depends on the withdrawals (*W*) and also on the distance (*H*) between the surface and the water table (piezometric)[4] level. Benefits from groundwater follow a linear water demand function (Gisser and Sánchez, 1980):

$$(2) \quad W = g + k \cdot P$$

with $g > 0$ and $k < 0$ being the equation parameters and *P* representing the volumetric water price. Following Gisser and Sánchez (1980), total benefits from groundwater consumption is the area under the inverse demand function ($P = \frac{1}{2k} \cdot W^2 - \frac{g}{k} \cdot W$).

[4] From hereafter we use "water table" and "piezometric" exchangeably.

On the other hand, pumping costs are linear, $C(W,H) = c_0' + c_1' \cdot (S_L - H)$, and represent the fixed costs of groundwater extraction (c_0') plus the marginal costs of groundwater pumped to the surface elevation (S_L). This expression can be simplified as:

(3) $C(W,H) = C_0 + C_1 \cdot H$

where $C_0 = c_0' + c_1' \cdot S_L$ and $C_1 = -c_1'$.

The social welfare maximization problem (*SW*) in Eq. (1) is subject to the dynamics of the groundwater resource. The aquifer water level (*H*) depends on the natural recharge (*R*) minus extractions (*W*).

(4) $H(t+1) = H(t) + (R - (1-\alpha)W) \cdot \frac{1}{AS}$

where AS is the total surface area of the aquifer (A) multiplied by the storativity factor (S), this is, the available volume of water that can be stored in the aquifer, and α represents the return flow rate. The temporal variable is *t*.

This model has been implemented in the economic literature (see review by Koundouri et al., 2017) to assess the optimal management of groundwater resources. However, while this model includes the extraction externality—the effect of groundwater depletion on increasing the pumping cost for all groundwater users, it does not consider other kinds of negative externalities associated with groundwater depletion. Several papers have included other externalities in this model to reflect possible impacts of groundwater depletion on related ecosystems (e.g., Roumasset and Wada, 2013; Esteban and Albiac, 2012; Esteban and Dinar, 2016), impacts on groundwater quality (e.g., Anderson et al., 1985; Roseta-Palma 2002), impacts on interaction between surface and groundwater bodies (e.g., Provencher, 1985; Tsur 1997; Kahil et al. 2015), among other interactions. In general, this literature demonstrates that with the inclusion of these types of impacts the efficient regulation of groundwater resources becomes a necessary policy.

However, to the best of our knowledge a proper groundwater management, including the development and impacts of land subsidence have not been analyzed. When considering land subsidence impacts, the groundwater management problem faces a notable change with respect to previous approaches. The magnitude of the land subsidence impacts together with their wider influence affect the previous social welfare function at least in two aspects. The first negative externality from subsidence involves negative impacts on infrastructures (damages to structures), impacts on human activities (agricultural yield reductions due to the sinking in the land or failure

of water-wells), and impacts on several ecosystems (environmental damages due to alteration in wetlands or groundwater related ecosystems, higher incidence of flooding risks, etc.). All these externalities are not accounted for, despite of the significant implications to the aggregated social welfare (SW). Second, there is another negative externality measured as the opportunity cost of losing reservoir storage capacity in the future (depending on the geological formation of the aquifer). The decrease in groundwater storage capacity aggravates previously mentioned impacts but also limits present water withdrawals. This second, land subsidence, impact can be very significant especially in arid and semi-arid regions, and also due to future water scarcity scenarios aggravated by climate change.

Therefore, taking into account these two externalities associated with land subsidence, the social welfare function in Eq. (1) can be expressed as:

$$(5) \quad SW^{LS} = \int_{t=0}^{\infty} e^{-it}[B\,(W) - C(W,H) - LS\,(W)]\,dt$$

where $LS\,(W)$ represents the social costs associated with land subsidence negative externality effects on infrastructure and human activity. This function depends on the land sinking/subsidence rate ($Sub\,(W)$) due to groundwater pumping. The land sinking is multiplied by the economic cost of this impact (β), measured in \$/m3 of subsidence, and it is assumed, for simplicity, to be a linear function. This function represents the economic costs, in terms of the impacts of land subsidence, per unit of groundwater withdrawals (m3).

$$(6) \quad LS(W) = \beta \cdot Sub\,(W)$$

Following Wade et al. (2018) the land subsidence bowl rate can be represented by:

$$(7) \quad Sub(W) = \rho \cdot W \cdot v \cdot b \cdot \sigma$$

where ρ is the fluid density (kg/m3), v is the acceleration due to gravity (m/s2), σ is the compressibility of the confining material (m-s2/kg), b is the thickness of the aquifer system (m) and W is the total groundwater extractions (m3). It is important to note that we hypothesize that this externality is uniformly distributed across the region and all pumping wells. While several authors stated that pumping externalities are heterogeneous in space and time (Loáiciga, 2004; Kuwayama and Brozovick, 2013; Merrill and Guilfoos, 2017; Wade et al., 2018), we assume, for simplicity and without a loss of generality, a single-cell aquifer with homogenous distribution of wells and impacts.

The model includes the second impact from land subsidence, namely the loss of aquifer storage capacity over time. Land subsidence impacts on aquifer storage are represented by the following equation of motion:

$$(8) \qquad \dot{H} = \begin{cases} (R - (1-\alpha)W) \cdot \dfrac{1}{AS} & if \quad t < t_C \\ (R - (1-\alpha)W) \cdot \dfrac{1}{\delta \cdot AS} & if \quad t \geq t_C \end{cases}$$

where δ is a constant ($0 < \delta \leq 1$) representing the impact of groundwater extraction on the storage capacity of the aquifer (storage capacity externality from land subsidence). In the model we assume, as is the case of ecosystem health functions (Esteban and Dinar 2016) that there is a critical water table (H_C) that once it is reached the land sinking takes places. This declining in the aquifer surface leads to a reduction in the storage capacity of the aquifer. For simplicity and without loss of generality we assume that this reduction is constant and does not depend on the volume of the aquifer. Additionally, as stated previously we assume a single-cell aquifer with homogenous wells and impacts.

Taking into account the two externalities from land subsidence the social planner problem is:

$$(9) \qquad \underset{W,t_c,H}{\text{Max}}\, SW^{LS} = \int_{t=0}^{t=t_c} e^{-it}[B\,(W) - C(W,H)]\,dt + \int_{t=t_c}^{\infty} e^{-it}[B\,(W) - C(W,H) - LS\,(W)]\,dt$$

$$s.t. \quad \dot{H} = \begin{cases} (R - (1-\alpha)W) \cdot \frac{1}{AS} & if \quad t < t_C \\ (R - (1-\alpha)W) \cdot \frac{1}{\delta \cdot AS} & if \quad t \geq t_C \end{cases}$$

$$H(t_0) = H_0\,; \qquad H(t_c) = H_C; \qquad t_c = free$$

Both the critical threshold (H_C) and the time at which this level is reached (t_C) are endogenously determined by the model.

Two-Stage optimal control resolution

The resolution of this optimal control problem requires the establishment of two phases (two-stage optimal control) problem by considering the two different states of the objective function and the equation of motion. This problem requires to backward-solve two separate Pontryagin problems

(Tomiyama, 1985; Tomiyama and Rossana, 1989; Makri, 2004; Aisa et al., 2007). Sub-problem 2 (SW_2^{LS}) which is firstly solved is:

$$(10) \qquad Max\ SW_2^{LS} = \int_{t=t_c}^{t=\infty} e^{-it}[B\ (W_2) - C(W_2, H_2) - LS\ (W_2)]\, dt$$

$$s.t. \quad \dot{H}_2 = \frac{[R+(\alpha-1)\cdot W_2]}{\delta \cdot AS}$$

$$H_2(t_c) = H_C; \qquad t_c\ and\ H_c\ given$$

The Hamiltonian of this problem is:

$$(11) \qquad \mathcal{H}_2(t, W_2, H_2, \lambda_2) = -e^{-it}[B\ (W_2) - C(W_2, H_2) - LS\ (W_2)] + \lambda_2 \cdot \frac{[R + (\alpha - 1) \cdot W_2]}{\delta \cdot AS}$$

with λ_2 being the costate variable, and W_2 and H_2 groundwater withdrawals and water table level respectively, under sub-problem 2. By solving the first order conditions and rearranging several terms we obtain the optimal results of this problem ($SW_2^{LS*}(H_c^*, t_c^*)$), and the optimal values of the state and control variables (W_2^* and H_2^*).

The complete development of sub-problem 2 is presented in the Appendix. The expressions of the optimal values of W_2^* and H_2^* are:

$$(12) \qquad W_2^*(t) = \left(H_C - \frac{NN - i \cdot \frac{MM}{mm}}{nn} \right) \cdot e^{-x_2(t-t_c)} - \frac{MM}{mm}$$

$$(13) \qquad H_2^*(t) = \left(H_C - \frac{NN - i \cdot \frac{MM}{mm}}{nn} \right) \cdot \frac{x_2}{mm} \cdot e^{-x_2(t-t_c)} - \frac{NN - i \cdot \frac{MM}{mm}}{nn}$$

with $mm = \frac{\alpha-1}{\delta \cdot AS}$, $nn = i \cdot k \cdot C_1$, $NN = -ig - i \cdot C_0 \cdot k - i \cdot \beta \cdot \rho \cdot v \cdot b \cdot \sigma \cdot k + \frac{C_1 \cdot k \cdot R}{\delta \cdot AS}$, and $MM = \frac{R}{\delta \cdot AS}$. Finally, the value of the co-state variable of sub-problem 2 is:

$$(14) \qquad \lambda_2^* = \frac{\delta \cdot AS}{\alpha - 1} \cdot e^{-it} \cdot \left[\frac{W_2}{k} - \frac{g}{k} - C_0 - C_1 \cdot H_2 - \beta \cdot \rho \cdot v \cdot b \cdot \sigma \right].$$

With the solution of sub-problem 2, we start solving sub-problem 1 (SW_1^{LS}):

$$(15) \qquad SW_1^{LS} = \int_{t=0}^{t=t_c} e^{-it}[B\ (W_1) - C(W_1, H_1)]\, dt + SW_2^{LS*}(H_c^*, t_c^*)$$

$$s.t. \quad \dot{H} = \frac{[R+(\alpha-1)\cdot W_1]}{AS}$$

$$H(t_0) = H_0\ ; \qquad H_1(t_c) = H_C; \qquad 0 \le t < t_c; \quad H_c\ is\ free\ and\ H_0\ is\ given$$

with $SW_2^{LS*}(H_c^*, t_c^*)$ being the optimal solution of sub-problem 2 and following Boucekkine et al. (2004), we impose the matching conditions of continuity and optimality:

$$(16) \qquad \lambda_1(t_c) = -\frac{\partial SW_2^{LS}(t_c, H_c)}{\partial H_c}$$

$$(17) \qquad \mathcal{H}_1^*(t_c, H_c) = \frac{\partial SW_2^{LS}(t_c, H_c)}{\partial t_c}$$

with $SW_2^{SL^*}$ and $SW_1^{SL^*}$ being the optimal solutions of the two sub-problems and $\mathcal{H}_1$ the Hamiltonian associated with sub-problem 1 (SW_1^{LS}):

$$(18) \qquad \mathcal{H}_1(t, W_1, H_1, \lambda_1) = -e^{-it}[B\,(W_1) - C(W_1, H_1)] + \lambda_1 \cdot \frac{[R + (\alpha - 1) \cdot W_1]}{AS}$$

where λ_1 is the costate variable and W_1 and H_1 are respectively groundwater withdrawals and water table level under sub-problem 1. Imposing the first order conditions and rearranging terms, the optimal solutions for sub-problem 1 are:[5]

$$(19) \qquad W_1^*(t) = A \cdot e^{y_1 \cdot t} + B \cdot e^{y_2 \cdot t} - \frac{M}{m}$$

$$(20) \qquad H_1^*(t) = \frac{m}{y_1} \cdot A \cdot e^{y_1 \cdot t} + \frac{m}{y_2} \cdot B \cdot e^{y_2 \cdot t} + \frac{N - i \cdot \frac{M}{m}}{n}$$

with $m = \frac{\alpha - 1}{AS}$, $M = \frac{R}{AS}$, $n = i \cdot k \cdot C_1$, $N = -ig - i \cdot C_0 \cdot k + C_1 \cdot k \cdot M$, and also

$B = \frac{y_2}{m}\left(H_c - \frac{N - i \cdot \frac{M}{m}}{n} - \frac{\left(H_c - \frac{N - i \cdot \frac{M}{m}}{n}\right) + \left(\frac{N - i \cdot \frac{M}{m}}{n} - H_0\right) \cdot e^{y_2 t_1}}{e^{y_1 t_1} - e^{y_2 t_2}} \right)$, and $A = \frac{\left(H_c - \frac{N - i \cdot \frac{M}{m}}{n}\right) + \left(\frac{N - i \cdot \frac{M}{m}}{n} - H_0\right) \cdot e^{y_2 t_1}}{\frac{m}{y_1}(e^{y_1 t_1} - e^{y_2 t_2})}$.

Numerical illustration: an economic interpretation of the optimal results

Previous solutions for the optimal control problem, stated in eq. 9, indicate how optimal paths for groundwater extractions and water table level are determined by land subsidence impacts. Land subsidence has a significant impact in both expressions of groundwater extractions and of water level, determining the optimal trajectories of these variables.

Optimal paths for groundwater withdrawals in presence of land subsidence can be summarized as:

[5] A complete development of the problem is presented in Appendix.

$$(21) \quad W^* = \begin{cases} A \cdot e^{y_1 \cdot t} + B \cdot e^{y_2 \cdot t} - \dfrac{M}{m} & \forall \quad t < t_c \\ \left(H_C - \dfrac{NN - i \cdot \dfrac{MM}{mm}}{nn} \right) \cdot e^{-x_2 (t - t_c)} - \dfrac{MM}{mm} & \forall \quad t \geq t_c \end{cases}$$

Additionally, the optimal paths of the water table level when considering land subsidence externalities are:

$$(22) \quad H^* = \begin{cases} \dfrac{m}{y_1} \cdot A \cdot e^{y_1 \cdot t} + \dfrac{m}{y_2} \cdot B \cdot e^{y_2 \cdot t} + \dfrac{N - i \cdot \dfrac{M}{m}}{n} & \forall \quad t < t_c \\ \left(H_C - \dfrac{NN - i \cdot \dfrac{MM}{mm}}{nn} \right) \cdot \dfrac{x_2}{mm} \cdot e^{-x_2 (t - t_c)} - \dfrac{NN - i \cdot \dfrac{MM}{mm}}{nn} & \forall \quad t \geq t_c \end{cases}$$

Due to the complexity of the expressions we cannot concisely interpret the impacts of all elements related with land subsidence in the theoretical results. To analyze the influence and interpret these parameters, we have performed a numerical illustration (over a horizon of 200 years—to allow reaching a steady state) using parameters from the Western La Mancha aquifer in Southeastern Spain. This numerical illustration has allowed us to come up with some conclusions on how the different land subsidence parameters determine the optimal paths of water extractions and water table level. Additionally, because the approximation of several parameters we have performed a sensitivity analysis with the main land subsidence parameters to better evaluate the impacts of subsidence on optimal groundwater management.

It is important to mention that the Western La Mancha aquifer is an aquifer with minimal to no land subsidence observed (Sanz, 2019). We illustrate the theoretical model behavior with this aquifer because the availability of hydrological and economic data (Esteban and Dinar, 2016; Esteban and Albiac, 2011), with additional approximated land subsidence parameters from Wade et al. (2018). Table 1 presents the parameters used for the numerical application.

Table 1. Values of Western La Mancha hydrological behavior and model parameters for private demand and ecosystem behavior function

Parameters	Description	Units	Value
k	Water demand slope	€/Mm3	−0.7272
g	Water demand intercept	€/Mm3	726.71
C_0	Pumping costs intercept	€/Mm3	319,500
C_1	Pumping costs slope	€/Mm3·m	−500
α	Return flow coefficient	-	0.2
H_0	Current water table	m	640
R	Natural recharge	Mm3	360
A	Aquifer area	km2	5,500
S	Storativity coefficient	-	0.0023
S_L	Surface elevation	m	665
i	Social discount rate	%	0.02
β	Economic Value of land subsidence	€/Mm3	2,085
ρ	Fluid density	kg/m3	1,000
v	Acceleration due to gravity	m/s2	9.81
b	Compressibility of the confined material	m-s2/kg	1·10-7
σ	Thickness of the confining unit	m	500
δ	Storage externality – Capacity Loss	-	0.9

Note: parameters from the aquifer and the economic equations are from Esteban and Dinar (2016), Esteban and Albiac (2011) and Frutos et al. (2019). The land subsidence parameters are from Wade et al. (2018).

Results

The first simulation (Figure 6) addresses a situation without land subsidence. This simulation assume that the storage externality is null ($\delta = 1$) and land subsidence externality is zero ($\beta = 0$). In this case, the results suggest that the water table level should increase from the current 640 meters until reaching 653 meters above sea level. This means that groundwater extractions should be negative during some years (which means an artificial recharge into the aquifer). The steady state will be reached after 80 years with a water table level of 653 meters above sea level.

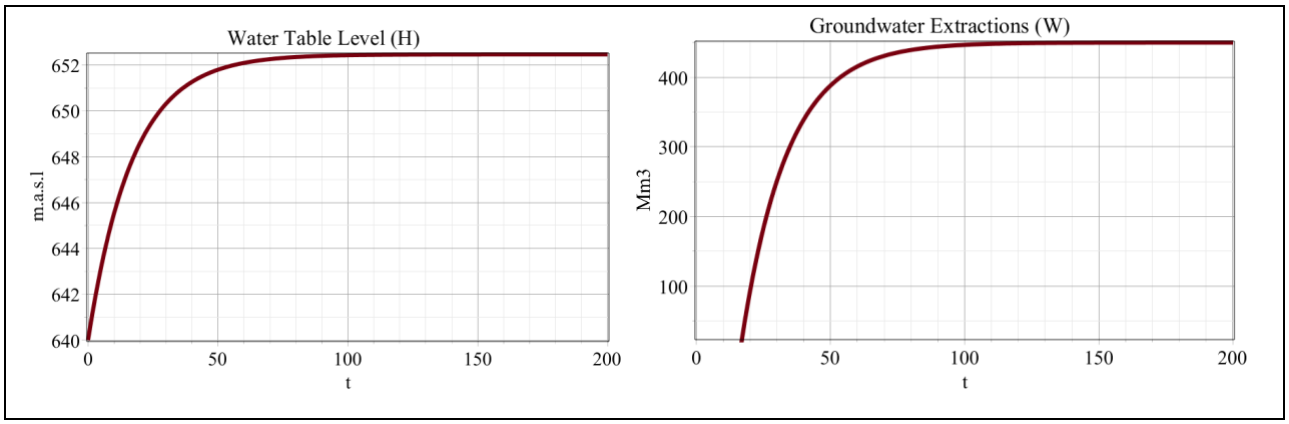

Figure 6. Water table and withdrawals in Western la Mancha aquifer: no land subsidence.
Source: Authors' elaborations.

However, when land subsidence problems are introduced to the model (see parameters in Table 1). The optimal results present a very different pattern (Figure 7). In this case, we can observe how in a first stage and until reaching the critical threshold, optimal groundwater extractions are negative. This means that the optimal paths suggest how the aquifer should be refilled until approximately year 12. After year 12, groundwater extractions should increase until reaching a yearly extraction of 620 Mm^3 in year 27. Finally, at year 28 the critical threshold is reached and withdrawals heavily fall again, the model suggests a refill of 400 Mm^3. The model stabilized in year 90 when the water table level has reached 656 meters above sea level.

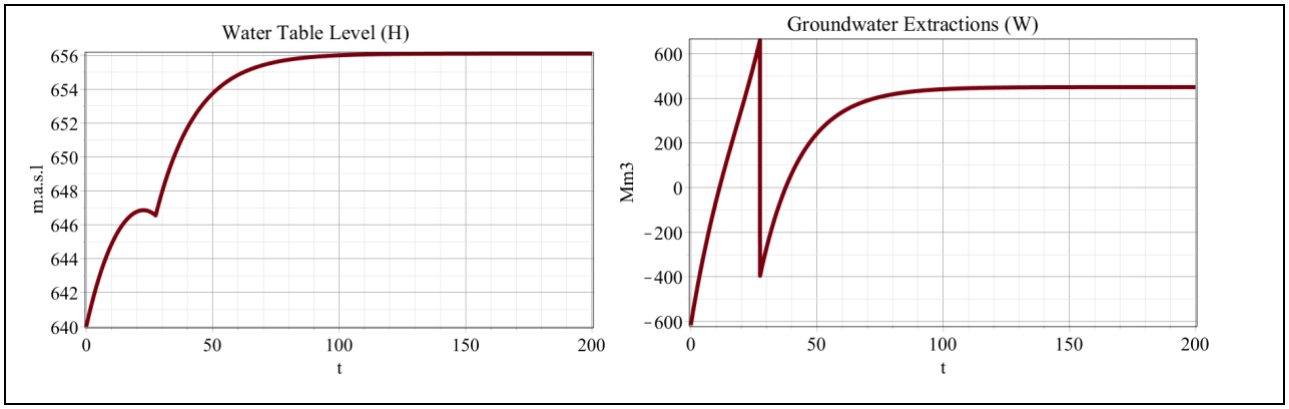

Figure 7. Water table and withdrawals in Western la Mancha aquifer: with land subsidence
Source: Authors' elaborations.

In order to analyze the impacts of land subsidence we have performed a sensitivity analysis with the main subsidence parameters. For simplicity, we have modified the land subsidence externality ($LS\ (W)$) by using the value of the economic impacts of land subsidence (β). Because all the parameters related to subsidence ($Sub\ (W)$) are multiplicative, the optimal expression contains them all. So, a modification of any of these parameters (Eqs. 6 and 7) has the same impact on the optimal solutions of the problem. The results presented in Figure 8 show how the optimal patterns are similar in all scenarios (higher and lower values of the land subsidence externality and also the baseline). However, differences exist in the optimal water table levels at the steady state, the stabilization time, and also the critical time at which the threshold is reached. The outcomes suggest that the higher the impact of the land subsidence the higher is the water table level at the steady state (658 vs. 655 meters above sea level). In addition, with larger land subsidence impacts the model stabilizes earlier. We can also observe how in the case of greater impacts of land subsidence the behavior of withdrawals is more extreme: The optimal paths suggest that higher refill levels are necessary, but also, groundwater extractions immediately after reaching the critical threshold level are much larger compared with having lower subsidence impacts.

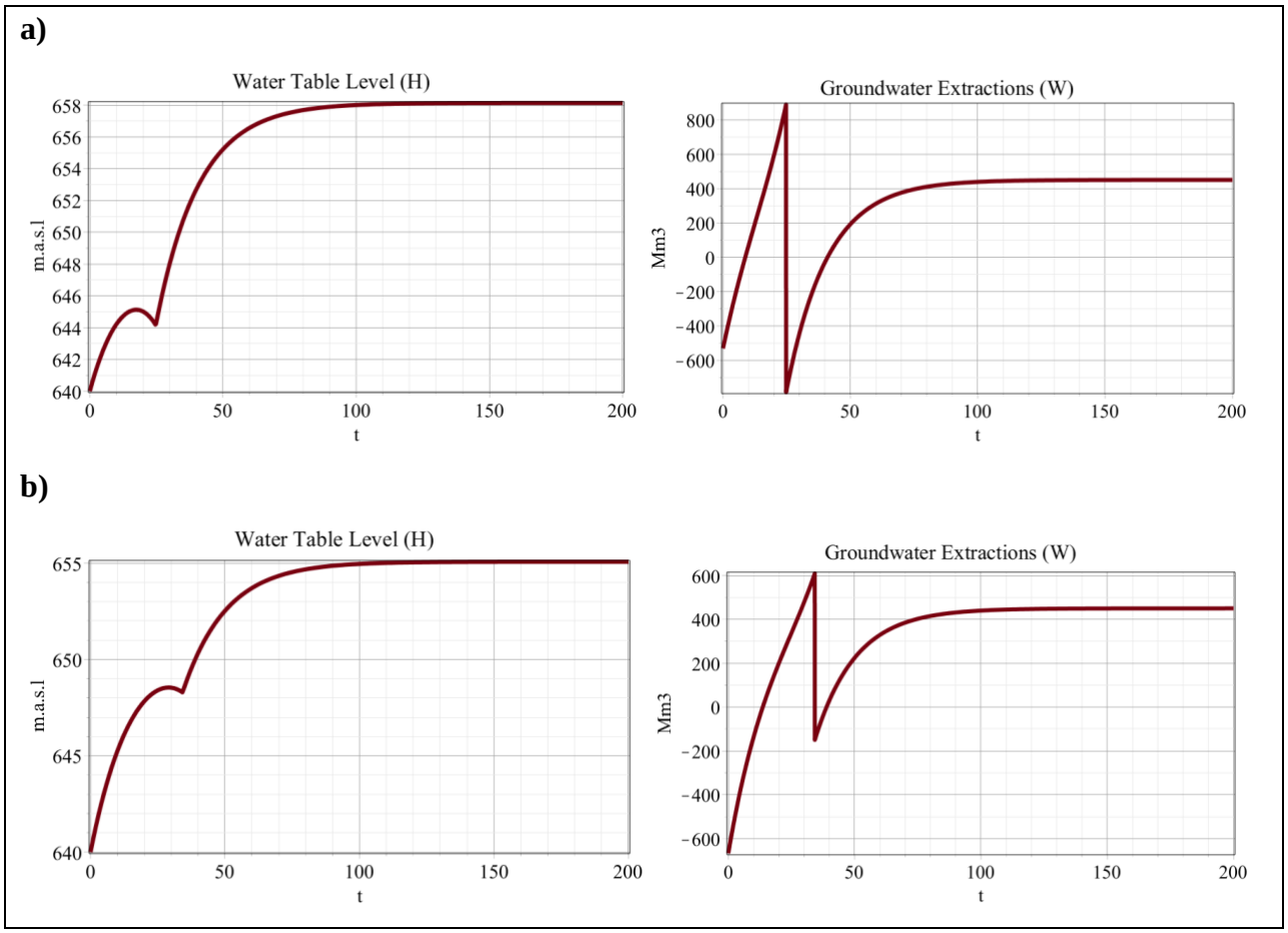

Figure 8. Sensitivity analysis: water table and withdrawals in Western la Mancha aquifer with higher and lower values of the land subsidence externality impact ($LS\,(W)$)

Note: a) represents the case of using higher values for the land subsidence externality impact (the externality impact has been doubled); b) represents the case of using lower values for the land subsidence externality impact (the externality impact has been cut by half).

Source: Authors' elaborations.

The final sensitivity analysis simulates the effect of the storage externality impact—the decrease in the aquifer capacity due to land subsidence. In this scenario we simulate a decrease in the aquifer capacity by an additional 10%.[6] The results presented in Figure 9 illustrate how the higher the storage externality the higher the impacts on the optimal water table and the groundwater pumping. Similar to the case of having a big land subsidence externality, under this scenario optimal water table level at the steady state is higher (658 meters). In addition,

[6] We assumed an initial storage externality of a 10% of loss in the aquifer capacity ($\delta = 0.9$).

groundwater pumping is associated with a larger variability, requiring a larger volume of refill but also with larger groundwater withdrawals after reaching the critical threshold.

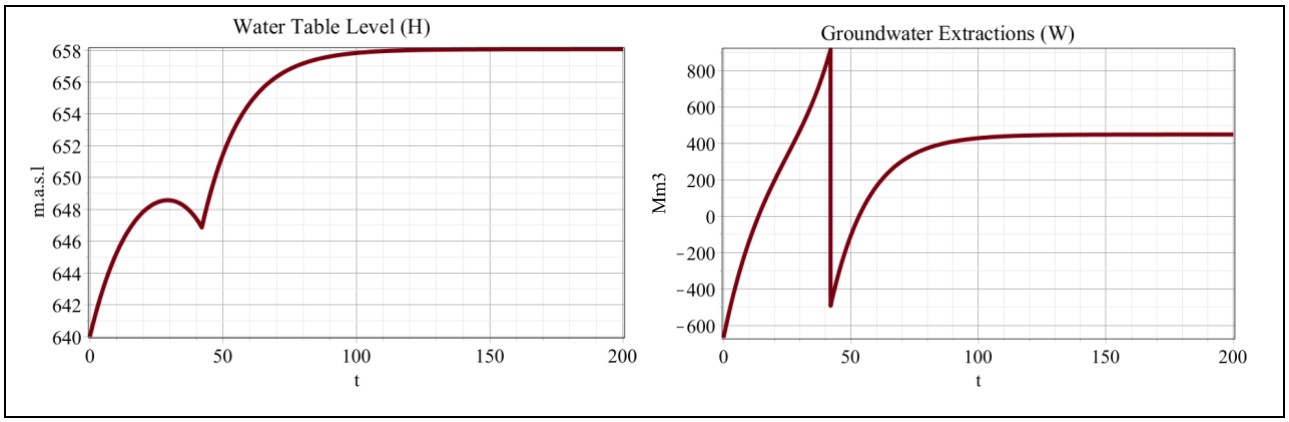

Figure 9. Sensitivity analysis: water table and withdrawals in Western la Mancha aquifer with higher storage externality (δ).
Source: Authors' elaborations.

Major results of the interaction between the land subsidence parameters and the main control (pumping rate) and state (water table level) variables can be summarized as follows:

Result 1. *The critical threshold* (H_C)*, which marks the water table level at which the system starts to subside, affects both groundwater extractions and the optimal water table level in both sub-periods. The higher the threshold the higher the value of the optimal water table level in both sub-periods.*

This result indicates how a high critical water table threshold level (meaning that overexploitation of the aquifer, will lead to land subsidence in an earlier stage) determines the optimal paths of the water table level in both sub-periods (sub problems 1 and 2). The higher the critical threshold level the faster is the water table level path reaching a steady state at the initial time period (sub-problem 1). In addition, the higher the critical threshold the higher the water table level at the steady state once the land has subsided. This result means that speed and level of steady state depend on the impacts of land subsidence along the time path during which the critical threshold will be reached. However, the higher this critical threshold level the longer the time to reach this level and also is the higher the water table level at the steady state.

Result 2. *Land subsidence externality ($LS(W)$) determines the final paths for groundwater extractions and optimal groundwater level. The higher the total economic impact of land subsidence the longer the time to stabilize the system.*

While it sounds trivial, this result indicates the sensitivity of the model to the level of damage caused by land subsidence to infrastructure and economic activity in the region. We expect that this result will also be sensitive to the value of the water use. The higher the value assigned to the water pumped, the less sensitive would the model be to the pumping impacts and thus, the higher is the decline in the water table and the extent of subsidence.

Result 3. *The larger the storage externality impact from land subsidence the lower is the rate of pumping and the lower is the decline in the water table.*

While it sounds trivial too, this result indicates the sensitivity of the model to the level of opportunity cost from loss of storage capacity to the region. We expect that this result will also be sensitive to the value of the water use in the region. A higher value assigned to the water pumped, the less sensitive would the model be to the pumping impacts and thus, the higher is the decline in the water table.

Result 4. *A large enough storage externality impact and/or a large enough land subsidence externality impact cause the model to never reach the second-stage (sub-problem 2). In this case, the optimal water table level would never reach the critical threshold and the steady state will be reached at a level higher than the critical threshold.*

This result suggests that there is a level of negative impact that will trigger the model in an optimal solution to prevent any irreversible damage (either in land subsidence impacts or in loss of storage capacity). In such cases the model downscales extractions to the level that they will not affect land subsidence and remain within what we defined as sub-problem 1.

Conclusion and Policy Implications

In spite of its major social cost in hundreds of locations around the world, the majority of which with irreversible negative physical and economic impacts, land subsidence has not been given proper preventive attention by regulatory agencies and local water management organizations in many countries. Damages in the range of billions of dollars have not been assessed. We were able

to identify land subsidence cases in 119 locations where mainly physical consequences of land subsidence have been accounted for but economic damages, likely in the range of billions of dollars, have not been assessed.

As a first step we developed a Land Subsidence Extent (LSE) index that relies on the occurrence of up to 10 land subsidence effects that were observed in these sites. While this approach may lead to a partial assessment of the impact of land subsidence across sites, this is at the moment the best approach to compare across sites under land subsidence impacts. One of our conclusions from this part of the analysis is that more resources and efforts are ought to be allocated by international agencies to the systematic and comparative analysis of drivers of land subsidence and measurements of land subsidence economics impacts.

The case studies that we present in this paper, that by no means are supposed to be representative of the physical situations facing all land subsidence sites—the economic activities that lead to over-pumping of groundwater, which results in many locations also in subsidence of the aquifer surface, and the policy interventions that have been used and showed various levels of success (or failure)—we may conclude that over-pumping that results from increase in economic activity, population growth and imbalance in water supply and demand in many regions, which may increase in severity in the future due to expected climate change effects, is a major determinant of the land subsidence that has occurred in these regions. One additional conclusion steaming from the case studies is that success of policy intervention can increase with an increased involvement of all sectors that are associated with the groundwater pumping and use.

Our paper brought us the need to develop an economic optimization model of groundwater use. In addition to previous groundwater economic optimization models that included only the externalities of water draw-down on the pumping cost and the effect on groundwater-dependent ecosystems, it includes also the negative externalities of infrastructure damages and the opportunity cost of aquifer storage loss. This model allowed us some preliminary illustrative analyses with conclusions that make us more confident in the need for economic analysis of land subsidence.

Some of the findings suggest a direct impact of the level of infrastructure damage on the optimal decisions of water pumping. The higher the total economic impact of land subsidence the longer the time to stabilize the system. A different conclusion vis a vis optimality is obtained in the case of the aquifer storage loss externality. The larger the storage externality impact from land

subsidence the lower is the rate of pumping and the lower is the decline in the water table. A final conclusion from our analysis of the optimal economic model addresses extreme damage levels. The model is very sensitive to high levels of land subsidence externalities. High enough storage externality impact and/or a large enough infrastructure land subsidence externality impact cause the model to never reach the second-stage (sub-problem 2). Instead, the optimal water table level would never reach the critical threshold and the steady state will be reached at a level higher than the critical threshold

Some additional analyses that we will conduct in next iterations of the paper will include different types of aquifers, the effect of the value of the water on the optimal pattern of the extraction, and the effects of future product price shocks and drought shocks on the pumping patterns.

References

Anderson, G., Opaluch, J., Sullivan, W.M. 1985. Nonpoint agricultural pollution: Pesticide contamination of groundwater supplies. *American Journal of Agricultural Economics*, 67: 1238-1246.

Antonioli, F., Anzidei,M., Amorosi, A., Lo Presti, V.,Mastronuzzi, G., Deiana, G., De Falco, G., Fontana, A., Fontolan, G., Lisco, S., Marsico, A., Moretti, M., Orrù, P.E., Sannino, G.M., Serpelloni, E., Vecchio, A., 2017. Sea-level rise and potential drowning of the Italian coastal plains: flooding risk scenarios for 2100. Quat. Sci. Rev. 158:29–43.

Aragón, R., Lambán, J., García-Aróstegui, J.L., Hornero, J. & Fernández-Grillo, A.I. 2006. Efectos de la explotación intensiva de aguas subterráneas en la ciudad de Murcia (España) en épocas de sequía: orientaciones para una explotación sostenible. *Boletín Geológico Y Minero*, 117:389-400.

Arvidsson, R. 2019. On the use of ordinal scoring scales in social life cycle assessment. *The International Journal of Life Cycle Assessment*, 24(3):604–606.

Aisa, R., Cabeza, J., and Larramona, G. 2007. Timing of migration. Economics Bulletin 6, 1-10.

Borchers Hames L. and Michael Carpenter. 2014. Land Subsidence from Groundwater Use in California. California Water Foundation, Summary Report, April.

Boucekkine, R., Saglam, C., and Vallée, T. 2004. Technology adoption under embodiment: A two-stage optimal control approach. Macroeconomic Dynamics 8, 250-271.

Corbau, C., U. Simeoni, C. Zoccarato, G. Mantovani and P. Teatini. 2019. Coupling land use evolution and subsidence in the Po Delta, Italy: Revising the past occurrence and prospecting the future management challenges, *Science of the Total Environment*, 654:1196-1208.

Carbognin, L., P. Teatini, L. Tosi, T. Strozzi and A. Tomasin, Present relative sea level rise in the Northern Adriatic coastal area. In: Marine Research at CNR, E. Brugnoli et al. eds., Consiglio Nazionale delle Ricerche, Dipartimento Terra e Ambiente, 1147-1162, 2011.

Chiang, A.C. 1999. *Elements of Dynamic Optimization*. Illinois: Waveland Press, INC.

Chino Basin Water Master – Administration. "Overview." Accessed November 22, 2019. http://www.cbwm.org/ov_administrat.htm.

Chino Basin Water Masters. 2007. "Management Zone 1 Subsidence Management Plan." Chino Basin Optimum Basin Management Program. 1-18.

Ciroth, A., and Franze, J. 2011. *LCA of an Eco-labelled Notebook—Consideration of Social and Environmental Impacts along the Entire Life Cycle*. Berlin: Green Delta TC GmbH.

Correggiari, A., Cattaneo, A., Trincardi, F., 2005. The modern Po Delta system: lobe switching and asymmetric prodelta growth. *Mar. Geol.* 222:49–74.

de Frutos Cachorro, J., Erdlenbruch, K., and Tidball, M. 2019. Sharing a groundwater resource in a context of regime shifts. *Environmental and Resource Economics* 72:913-940.

Doglioni, C. (1993), Some remarks on the origin of foredeeps, Tectonophysics, 228, 1–20, doi:10.1016/0040-1951(93)90211-2.

Erban, Laura E., Steven M. Gorelick, Howard A. Zebker, and Scott Fendorf. "Release of arsenic to deep groundwater in the Mekong Delta, Vietnam, linked to pumping-induced land subsidence." Proceedings of the National Academy of Sciences 110, no. 34 (2013): 13751-13756.

Erkens, G., M.J. van der Meulen and H. Middelkoop (2016). Double trouble: subsidence and CO2 respiration due to 1,000 years of Dutch coastal peatlands cultivation. *Hydrogeology Journal*, 24, 551-568, doi: 10.1007/s10040-016-1380-4.

Fontes, J. 2016. *Handbook for Product Social Impact Assessment* Version 3.0. Amersfoort: PRé Sustainability.

French, James J. Ground-water outflow from Chino basin, upper Santa Ana valley, southern California. US Government Printing Office, 1972.

Isotton, G., P. Teatini, M. Ferronato, C. Janna, N. Spiezia, S. Mantica and G. Volonte. 2019. A robust numerical implementation of a 3D rate-dependent model for reservoir geomechanical simulations, *International Journal for Numerical and Analytical Methods in Geomechanics*, 1-20, doi:10.1002/nag.3000, 2019.

Galassi, G.; Levarlet, F. 2017. Improving sustainability of programmes in strategic environmental assessment procedures: The QUAlitative Structural Approach for Ranking (QUASAR) the environmental effects. *European Journal of Sustainable Development*, 6(1):233-246–246.

Gambolati, G. and P. Teatini. 2015. Geomechanics of subsurface water withdrawal and injection. *Water Resources Research*, *51*(6):3922-3955.

Heri, A., H. Z. Abidin, D. A. Sarsito, and D. Pradipta. 2018. Adaptation of 'early climate change disaster' to the northern coast of Java Island Indonesia, *Engineering Journal*, 22(3):207-219.

Herrera, G., J.A., Fernández, R. Tomás, G. Cooksley, and J. Mulas. 2009a. Advanced interpretation of subsidence in Murcia (SE Spain) using A-DInSAR data – modelling and validation. Nat. Hazards Earth Syst. Sci., 9, 647-661, doi: 10.5194/nhess-9-647-2009.

Herrera, G., R. Tomás, J.M. Lopez-Sanchez, J. Delgado, F. Vicente, J. Mulas, G. Cooksley, M. Sanchez, J. Duro, A. Arnaud, P. Blanco, S. Duque, J.J., Mallorqui, R. De la Vega-Panizo, and O. Monserrat. 2009b. Validation and comparison of Advanced Differential Interferometry Techniques: Murcia metropolitan area case study. ISPRS Journal of Photogrammetry and Remote Sensing, 64, 501-512.

Holzer, T.L. and D.L. Galloway (2005). Impacts of land subsidence caused by withdrawal of underground fluids in the United States. *Reviews in Engineering Geology* 2005, XVI:87-99.

Hosseinijou, S., S. Mansour, and M. Shirazi. 2014. Social life cycle assessment for material selection: A case study of building materials. *International Journal of Life Cycle Assessment*, 19(3):620–645.

IGME, 2000. Estudio geotécnico del subsuelo del área metropolitana de Murcia. Instituto geológico y Minero de España y Consejería de Obras Públicas y Ordenación territorial de la Región de Murcia. Internal report, 120 pp (in Spanish).

Jones, L. L. and J. Larson. 1975. Economic Effects if Land Subsidence Due to Excessive Groundwater Withdrawal in the Texas Gulf Coast Area. Texas Water Resources Institute TR-67 1975.

Kahil, T., Ward, F., Albiac, J., Eggleson, J., and Sanz, D. 2015. Hydro-economic modeling with aquifer–river interactions to guide sustainable basin management. Journal of Hydrology 539, 510-524.

Koundouiry, P., Roseta-Palma, C., and Englezo, N. 2017. Out of sight, not out of mind: developments in economic models of groundwater management. International review of environmental and resource economics 11, 55-96.

Kuwayama Y. and Brozovic N. 2013. The regulation of spatially heterogeneous externality: Tradable groundwater permits to protect streams. Journal of Environmental Economics and Management 66, 364-382.

Lixin, Y., W. Jie, S. Chuanqing, J. Guo, J. Yanxiang and B. Liu (2010). Land Subsidence Disaster Survey and Its Economic Loss Assessment in Tianjin, China. *Natural Hazards Review*, 11, 35-41, doi: doi:10.1061/(ASCE)1527-6988(2010)11:1(35).

Loáiciga H.A. 2004. Analytic game – theoretic approach to ground-water extraction. Journal of Hydrology 297, 22-33.

Makris, M. 2001. Necessary conditions for infinite-horizon discounted two-stage optimal control problems. Journal of Economic Dynamics and Control 25, 1935-1950.

Martínez-Blanco, J.; Lehmann, A.; Muñoz P., et al. 2014. Application challenges for the social life cycle assessment of fertilizers within life cycle sustainability assessment. *Journal of Clean Production*, 69:34–48.

Mattavelli, L., T. Ricchiuto, D. Grignani, and M. Schoell (1983), Geochemistry and habitat of natural gases in Po basin, northern Italy, Am. Assoc. Pet. Geol. Bull., 67(12), 2239–2254.

Merrill N.H. and Guilfoos T. 2017. Optimal groundwater extraction under uncertainty and spatial stock externality. Americal Journal of Agricultural Economics 100(1), 220-238.

Mulas, J., Aragón, R., Martínez, M., Lambán, J., García-Aróstegui, J.L., Fernández-Grillo, A.I., Hornero, J., Rodríguez, J. & Rodríguez, J.M. 2003. Geotechnical and hydrogeological analysis of land subsidence in Murcia (Spain). Materials and Geoenvironment, 50, 249-252.

Provencher B. 1985. Issues in the conjunctive use of surface water and groundwater. D. Bromley (Ed.), The Handbook of Environmental Economics, Blackwell Sci, Oxford.

Ramirez, P.K.; Petti, S.L.; Haberland, N.T.; Ugaya, C.M.L. 2014. Subcategory assessment method for social life cycle assessment. Part 1: Methodological Framework. *International Journal of Life Cycle Assessment*, 19(8):1515–1523.

Roseta-Palma, C. 2002. Groundwater Management When Water Quality Is Endogenous. Journal of Environmental Economics and Management 44(1), 93-105.

Roumasset, J., and Wada, C. 2013. A dynamic approach to PES pricing and finance for interlinked ecosystem services: Watershed conservation and groundwater management. Ecological Economics 87, 24-33.

Sanz, D. 2019. Personal Communication, April 14 2019.

Simeoni, U., Corbau, C., 2009. A review of the Delta Po evolution (Italy) related to climatic changes ad human impacts. In: Corbau, C., Simeoni, U. (Eds.), Special Issue Coastal Vulnerability Related to Sea-level Rise. Geomorphology vol. 107 (1–2), pp. 64–71.

Syvitski, J.P.M., Kettner, A.J., Overeem, I., Hutton, E.W.H., Hannon, M.T., Brakenridge, G.R., Day, J., Vörösmarty, C., Siato, Y., Giosan, L., Nicholls, R., 2009. Sinking deltas due to human activities. Nat. Geosci. 2, 681–686.

Teatini, P., L. Tosi, and T. Strozzi, Quantitative evidence that compaction of Holocene sediments drives the present land subsidence of the Po Delta, Italy, Journal of Geophysical Research - Solid Earth , 116, B08407, doi:10.1029/2010JB008122, 2011.

Tessitore, S., Fernández-Merodo, J.A., Herrera, G., Tomás, R., Ramondini, M., Sanabria, M., Duro, J., Mulas, J. & Calcaterra, D. 2016. Comparison of water-level, extensometric, DInSAR and simulation data for quantification of subsidence in Murcia City (SE Spain). Hydrogeology Journal, 24, 727-747, doi: 10.1007/s10040-015-1349-8.

Thomas B.F. and Famiglietti J.S. 2019. Identifying Climate-Induced Groundwater Depletion in GRACE Observations. Scientific Report 9, 4124.

Tomás, R., Domenech, C., Mira, A., Cuenca, A. & Delgado, J. 2007. Preconsolidation stress in the Vega Baja and Media areas of the River Segura (SE Spain): Causes and relationship with piezometric level changes. Engineering Geology, 91, 135-151.

Tomás, R., Herrera, G., Cooksley, G. & Mulas, J. 2011. Persistent Scatterer Interferometry subsidence data exploitation using spatial tools: The Vega Media of the Segura River Basin case study. *Journal of Hydrology*, 400, 411-428.

Tomás, R., Herrera, G., Delgado, J., Lopez-Sanchez, J.M., Mallorquí, J.J. & Mulas, J. 2010. A ground subsidence study based on DInSAR data: Calibration of soil parameters and subsidence prediction in Murcia City (Spain). *Engineering Geology*, 111, 19-30.

Tomás, R., Márquez, Y., Lopez-Sanchez, J.M., Delgado, J., Blanco, P., Mallorquí, J.J., Martínez, M., Herrera, G. & Mulas, J. 2005. Mapping ground subsidence induced by aquifer overexploitation using advanced Differential SAR Interferometry: Vega Media of the Segura River (SE Spain) case study. *Remote Sensing of Environment*, 98, 269-283.Tomiyama, K. 1985. Two-stage optimal control problems and optimality conditions. Journal of Economic Dynamics and Control 9, 317-337.

Tomiyama, K., and Rossana, R.J. 1989. Two-stage optimal control problems with an explicit switch point dependence. Journal of Economic Dynamics and Control 13, 319-337.

Tsur Y. 1997. The economics of conjunctive ground and surface water irrigation systems: Basic principles and empirical evidence from Southern California. D. Parker, Y. Tsur (Eds.), Decentralization and Coordination of Water Resource Management, Kluwer Academic, Dordrecht.

Wade C.M., Coborun K.M., Amacher G.S. and Hester E.T. 2018. Policy targeting to reduce economic damages from land subsidence. Water Resource Research 54, 4401-4416.

Warren, John P., Lonnie L. Jones, Ronald D. Lacewell, and Wade L. Griffin. 1975. External Costs of Land Subsidence in the Huston-Baytown Area. *American Journal of Agricultural Economics*, 57(3):450-455.

Wildermuth Environmental Inc. 2015. 2014 Annual Report of Ground-Level Monitoring Committee.

Wildermuth Environmental Inc. 2016. 2015 Annual Report of Ground-Level Monitoring Committee.

Wildermuth Environmental Inc. 2017. 2016 Annual Report of Ground-Level Monitoring Committee.

Wildermuth Environmental Inc. 2018. 2017 Annual Report of Ground-Level Monitoring Committee.

Wildermuth Environmental Inc. 2002. Chino Basin Optimum Basin Management Program. Initial State of the Basin Report. In: Chino Basin Water Masters Engineering Reports, pp. 1-141.

Wildermuth, M. J., J. P. LeClaire, A. E. Malone, J. H. Hwang, J. V. Rossi, and R. Atwater. 2005. Chino Basin optimum basin management program. In Managing Watersheds for Human and Natural Impacts: Engineering, Ecological, and Economic Challenges, pp. 1-12.

Yoo, J., and C. Perrings (2017). An externality of groundwater depletion: land subsidence and residential property prices in Phoenix, Arizona, *Journal of Environmental Economics and Policy*, 6(2):121-133, DOI: 10.1080/21606544.2016.1226198.

Appendix: Development of the Phase 2 Optimal Control Problem

The Hamiltonian (eq. (11)) corresponding with the second sub-problem can be stated as follows,

$$(A1) \qquad \mathcal{H}_2(t, W_2, H_2, \lambda_2) = -e^{-it}\left[\frac{W_2^2}{2\cdot k} - \frac{g}{k}W_2 - (C_0 + C_1 \cdot H_2)W_2 - \beta \cdot \rho \cdot v \cdot b \cdot \sigma \cdot W_2\right] + \lambda_2 \cdot \frac{[R + (\alpha - 1)\cdot W_2]}{\delta \cdot AS}$$

The first order conditions (FOC) are,

$$(A2) \qquad \frac{\partial \mathcal{H}_2}{\partial W_2} = -e^{-it}\left[\frac{1}{k}\cdot W_2 - \frac{g}{k} - C_0 - C_1 \cdot H_2 - \beta \cdot \rho \cdot v \cdot b \cdot \sigma\right] + \lambda_2 \cdot \left(\frac{\alpha - 1}{\delta \cdot AS}\right) = 0$$

from this equation we obtain the value of the costate variable λ_2,

$$(A3) \qquad \lambda_2 = \frac{\delta}{m}\cdot e^{-it}\left[\frac{1}{k}\cdot W_2 - \frac{g}{k} - C_0 - C_1 \cdot H_2 - \beta \cdot \rho \cdot v \cdot b \cdot \sigma\right]$$

with $m = \frac{\alpha - 1}{AS}$.

$$(A4) \qquad -\frac{\partial \mathcal{H}_2}{\partial H_2} = \dot{\lambda_2}$$

Solving this derivative and replacing $\dot{\lambda_2}$ by its differential with respect to time (from eq. (A3)) we obtain,

$$(A5) \qquad -C_1 \cdot W_2 = \frac{\delta}{m}\left[\frac{-i}{k}\cdot W_2 + \frac{i\cdot g}{k} + i \cdot C_0 + i \cdot C_1 \cdot H_2 + i \cdot \beta \cdot \rho \cdot v \cdot b \cdot \sigma - \frac{C_1 \cdot R}{\delta \cdot AS} - C_1 \frac{m}{\delta} W_2 + \frac{\dot{W_2}}{k}\right]$$

$$(A6) \qquad \dot{H_2} = \frac{R + (\alpha - 1)\cdot W_2}{\delta \cdot AS}$$

Finally, the transversality condition,

$$(A7) \qquad \lim_{t\to\infty} \lambda_2(t) = 0$$

Substituting the value of $\dot{H_2}$ in previous eq. (A6), into eq. (A5) and rearranging terms we get the following expression,

$$(A7) \qquad \dot{W_2} = i \cdot W_2 - i \cdot C_1 \cdot k \cdot H_2 + \left(-i \cdot g - i \cdot k \cdot C_0 - i \cdot \beta \cdot \rho \cdot v \cdot b \cdot \sigma \cdot k + \frac{k \cdot C_1 \cdot R}{\delta \cdot AS}\right)$$

Additionally, the value of $\dot{H}_2$ can be expressed as,

$$(A8) \qquad \dot{H}_2 = \frac{(\alpha - 1) \cdot W_2}{\delta \cdot AS} + \frac{R}{\delta \cdot AS}$$

The general solution of this system of two differential equations (eqs. A7 and A8) is,

$$(A9) \qquad W_2^*(t) = \left(H_C - \frac{NN - i \cdot \frac{MM}{mm}}{nn} \right) \cdot \frac{x_2}{mm} \cdot e^{x_2(t - t_c)} - \frac{MM}{mm}$$

$$(A10) \qquad H_2^*(t) = \left(H_C - \frac{NN - i \cdot \frac{MM}{mm}}{nn} \right) \cdot e^{x_2(t - t_c)} - \frac{NN - i \cdot \frac{MM}{mm}}{nn}$$

with $mm = \frac{\alpha - 1}{\delta \cdot AS}$, $nn = i \cdot k \cdot C_1$, $NN = -ig - i \cdot C_0 \cdot k - i \cdot \beta \cdot \rho \cdot v \cdot b \cdot \sigma \cdot k + \frac{C_1 \cdot k \cdot R}{\delta \cdot AS}$, and finally $MM = \frac{R}{\delta \cdot AS}$. Finally, the value of the costate variable of sub-problem 2 is,

$$(A11) \qquad \lambda_2^* = \frac{\delta \cdot AS}{\alpha - 1} \cdot e^{-it} \cdot \left[\frac{W_2}{k} - \frac{g}{k} - C_0 - C_1 \cdot H_2 - \beta \cdot \rho \cdot v \cdot b \cdot \sigma \right]$$

With the solution of sub-problem 2 (SW_2^{LS*}) we can state sub-problem 1 (eq. 14):

$$(A12) \qquad SW_1^{LS} = \int_{t=0}^{t=t_c} e^{-it} \left[\frac{W_1^2}{2 \cdot k} - \frac{g}{k} W_1 - (C_0 + C_1 \cdot H_1) \cdot W_1 \right] dt + SW_2^{LS*}(H_c^*, t_c^*)$$

$$s.t. \quad \dot{H} = \frac{[R + (\alpha - 1) \cdot W_1]}{AS}$$

$$H(t_0) = H_0 ; \qquad H_1(t_c) = H_C; \qquad 0 \le t < t_c; \quad H_c \; is \; free \; and \; H_0 \; is \; given$$

The Hamiltonian of this sub-problem is expressed as:

$$(A13) \qquad \mathcal{H}_1(t, W_1, H_1, \lambda_1) = -e^{-it}[B\,(W_1) - C(W_1, H_1)] + \lambda_1 \cdot \frac{[R + (\alpha - 1) \cdot W_1]}{AS}$$

where λ_1 is the costate variable of this sub-problem.

The first order conditions (FOC) are:

$$(A14) \qquad \frac{\partial \mathcal{H}_1}{\partial W_1} = -e^{-it} \left[\frac{W_1}{k} - \frac{g}{k} - C_0 - C_1 \cdot H_1 - \beta \cdot \rho \cdot v \cdot b \cdot \sigma \right] + \lambda_1 \cdot \left(\frac{\alpha - 1}{AS} \right) = 0$$

$$(A15) \quad \frac{\partial \mathcal{H}_1}{\partial H_1} = -\dot{\lambda_1}$$

$$(A16) \quad \frac{\partial \mathcal{H}_1}{\partial \lambda_1} = \dot{H_1} = \frac{[R + (\alpha - 1) \cdot W_1]}{AS}$$

From eq. A14 we can obtain the expression for λ_1,

$$(A17) \quad \lambda_1 = \frac{AS}{\alpha - 1} \cdot e^{-it} \cdot \left[\frac{W_1}{k} - \frac{g}{k} - C_0 - C_1 \cdot H_1 - \beta \cdot \rho \cdot v \cdot b \cdot \sigma\right]$$

By differentiating this equation, we obtain,

$$(A18) \quad \dot{\lambda}_1 = \frac{AS}{\alpha - 1} \cdot e^{-it} \cdot \left[-i \cdot \left(\frac{W_1}{k} - \frac{g}{k} - C_0 - C_1 \cdot H_1 - \beta \cdot \rho \cdot v \cdot b \cdot \sigma\right) + \frac{\dot{W}_1}{k} - C_1 \cdot \dot{H}_1\right]$$

With eq. A18 and eq.16 we can rewrite the problem as a system of two differential equations:

$$(A19) \quad \begin{pmatrix} \dot{W}_1 \\ \dot{H}_1 \end{pmatrix} = \begin{pmatrix} i & - \\ m & 0 \end{pmatrix} \cdot \begin{pmatrix} W_1 \\ H_1 \end{pmatrix} + \begin{pmatrix} N \\ M \end{pmatrix}$$

with $m = \frac{\alpha - 1}{AS}$, $n = i \cdot k \cdot C_1$, $N = -i \cdot g - i \cdot k \cdot C_0 - \beta \cdot \rho \cdot v \cdot b \cdot \sigma + C_1 \cdot k \cdot \frac{R}{AS}$, and $M = \frac{R}{AS}$.

The particular solutions of this system of differential equations are,

$$(A20) \quad W_1^*(t) = A \cdot e^{y_1 \cdot t} + B \cdot e^{y_2 \cdot t} - \frac{M}{m}$$

$$(A21) \quad H_1^*(t) = \frac{m}{y_1} \cdot A \cdot e^{y_1 \cdot t} + \frac{m}{y_2} \cdot B \cdot e^{y_2 \cdot t} + \frac{N - i \cdot \frac{M}{m}}{n}$$

with y_1 and y_2 being the roots of the differential equations' systems $\left(y_1 = \frac{i + \sqrt{i^1 - 4nm}}{2}\right.$ and $\left. y_2 = \frac{i - \sqrt{i^1 - 4nm}}{2}\right)$. Finally, constants A and B are determined by imposing the initial conditions of the problem ($H_1(t_0) = H_0$ and $H_1(t_c) = H_C$. The expressions for these constants are,

$$(A23) \quad B = \frac{y_2}{m}\left(H_c - \frac{N - i \cdot \frac{M}{m}}{n} - \frac{\left(H_c - \frac{N - i \cdot \frac{M}{m}}{n}\right) + \left(\frac{N - i \cdot \frac{M}{m}}{n} - H_0\right) \cdot e^{y_2 t_1}}{e^{y_1 t_1} - e^{y_2 t_2}}\right)$$

$$(A24) \quad A = \frac{\left(H_c - \frac{N - i \cdot \frac{M}{m}}{n}\right) + \left(\frac{N - i \cdot \frac{M}{m}}{n} - H_0\right) \cdot e^{y_2 t_1}}{\frac{m}{y_1}(e^{y_1 t_1} - e^{y_2 t_2})}$$

The principle of maximum provides necessary conditions for optimality, but it is necessary to verify that the second order conditions are also verified. The compliance of the second order conditions guarantees that the necessary conditions provided by the maximum principle are also sufficient for global optimality. A basic sufficiency theorem that guarantees the second order conditions was stated by Mangasarian (Chiang 1992, pp. 214-217). In this problem, it can be verified that the sufficient conditions of the Mangasarian theorem are verified, so we can state that the trajectories calculated are optimal.